ELSEVIER

Journal of Nuclear Materials 313–316 (2003) 1056–1060

journal of nuclear materials

www.elsevier.com/locate/jnucmat

Modeling approach to a 3D simulation of transport in TEXTOR-DED laminar zone with a finite element method

M. Kobayashi [a,*], D. Reiser [a], G. Sewell [b], K.H. Finken [a], S.S. Abdullaev [a]

[a] *Institut für PlasmaPhysik, Forschungszentrum Jülich GmbH, Euratom Association, TEC 52425 Jülich, Germany*
[b] *Department of Mathematics, University of Texas at El-Paso, Texas TX 79968, USA*

Abstract

A modeling approach to 3D transport simulations for an edge ergodized plasma with a finite element method coupled with a finite difference method is discussed. The idea of the modeling is based on a laminar zone, where one can approximate the transport with scrape-off layer model. The topics to be discussed are an optimization of 3D grids, a problem with CPU time (slow down of the code), and accuracy of the code as checked with a particle balance.
© 2003 Elsevier Science B.V. All rights reserved.

Keywords: 3D transport modeling; Laminar zone; Finite element method; Finite difference method; MHD equation

1. Introduction

In order to predict a heat load pattern onto the wall materials, a modeling of the plasma transport in an ergodic region is a very important topic for TEXTOR-dynamic ergodic divertor (DED) [1]. Up to now there have been 1D and 2D modeling approaches for this problem. These efforts contain several approximations which are very questionable for the plasma edge. The magnetic field lines are a mixture of ergodic field lines with a long connection length between two intersections with the wall and a laminar zone, where the connection length is relatively short. Therefore 3D modeling is essential. At the moment several modelings have been tested such as finite element [2], finite difference [3] and Monte Carlo methods [4,5]; each of these schemes has its own advantages and disadvantages.

The purpose of this paper is to discuss a modeling approach to 3D transport simulations in an edge ergodized plasma with a finite element method (FEM), giving practical examples in numerics and pointing out the problems to be solved. Although the analysis is based on the configuration of TEXTOR-DED, the discussion here will not lose generality and can be extended to all other cases.

The paper consists as follows. The basic ideas of the modeling are described in Section 2. In Section 3, several topics about numerical implementation are presented and discussed. A summary is given in Section 4.

2. An idea of the modeling

The details of the DED configuration and of the magnetic field structure are found in [1,6]. Here we briefly describe the idea of the modeling.

As mentioned in Section 1, the magnetic field structure is three dimensional at the edge. The idea is that the laminar zone plays an important role at the final step of the transport to the wall and in such a short connection length region a normal scrape-off layer (SOL) model is available. Thus the modeling concentrates on the laminar zone. In the following discussion, for the measure of connection length we use the number of poloidal turns that the flux tube experiences before hitting the wall, instead of length unit. One poloidal turn corresponds to about 30 m.

Because of the localization of the perturbation at high field side (HFS), the majority of field lines hit the wall there as shown in Fig. 1. Therefore, there are two

[*] Corresponding author. Tel.: +49-2461 613424; fax: +49-2461 612970.
E-mail address: m.kobayashi@fz-juelich.de (M. Kobayashi).

0022-3115/03/$ - see front matter © 2003 Elsevier Science B.V. All rights reserved.
PII: S0022-3115(02)01537-4

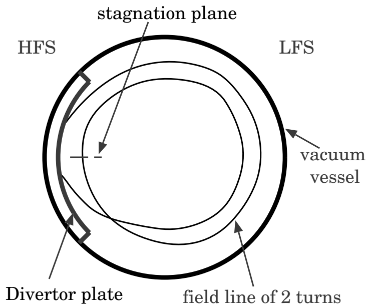

Fig. 1. An example of two poloidal turn field lines, where the trajectory is projected onto a certain poloidal cut. In this case the symmetric plane (stagnation plane) exits at HFS as shown with the broken line. For odd number of poloidal turns, the symmetric plane is located at LFS.

locations (cuts) of the highest symmetry, a cut near the outer mid-plane and near the inner mid-plane. In these two cuts one expects stagnation points of the convective flow, namely, at the low field side (LFS) for an odd number of poloidal turns and at HFS for an even number of turns. In this way, the picture of the transport at the edge is rather simplified.

3. Numerical realization

3.1. Grids

The numerical scheme investigated here is based on a splitting method, and consists of a FEM [7] for cross field transport and a finite difference method (FDM) for parallel transport. At each time step, the FEM and the FDM are alternated. The cross field transport is approximated on poloidal cross sections at each 90° toroidal angle, which is triangulated for the FEM. The triangles on each poloidal cut are connected in order to obtain volume cells for the FDM in the parallel direction. In order to reflect the three dimensional structure of the magnetic field, the volume cells are oriented along the flux tubes. This is done by mapping the grid along field lines over the whole computation domain. In this way, each volume cell represents a flux tube, and we call such grids 3D grids.

This is, however, not so easily done because the triangles tend to overlap each other after the mapping for certain distance due to the deformation of the flux tube [2]. This 'crushing' on one hand side is a numerical artifact. The mapping of flux tubes is area preserving. However, in a chaotic system the flux tubes can be strongly elongated and bent such that the triangle cells used in the FEM loose their straight character. If one connects the triangle vertices by lines, the triangles do not preserve area and even may overlap. However, considering the location of the strongest stretching and bending, one can find an optimized scheme as shown in Fig. 2. Here the case of the two poloidal turns is considered. The stagnation zone (Fig. 2(b)) is first mapped until the flux tube is highly deformed (Fig. 2(a)). In this cut an enough number of lines to resolve the deformation is introduced and mapped back to the stagnation area. Because of the symmetry of the problem, a symmetric set of lines is added there (Fig. 2(c)). The squares thus generated are subdivided into triangles (Fig. 2(d)). The triangles are now fine enough to follow the deformation, so that the grid is optimized not to overlap, as shown in Fig. 3.

The optimization was checked with the area preservation of each triangle. We made several tries for each region to reduce the error in area, but the best is around 10%, which will result in the error of flux conservation of particles, energy and momentum. The whole area of the bunch of flux tubes, on the other hand, is well preserved within less than 1% error. The validity of the grid has to be discussed concerning what quantity we need to calculate.

3.2. CPU time

Saving CPU time is one of the major issues for a large computation, and we first checked this as well as convergence of the code, starting with as simple a geometry as possible. A straight SOL of 10 m long was assumed with a square cross section $(\Delta x, \Delta y) = (2, 4)$ cm, where in Cartesian coordinate (x, y, z), z is along field lines, x and y are perpendicular each other and to the field lines. We solved Braginskii equations [8] in the following form (all notations are standard ones);

$$\frac{\partial n}{\partial t} = \frac{\partial}{\partial x}\left(D\frac{\partial n}{\partial x}\right) + \frac{\partial}{\partial y}\left(D\frac{\partial n}{\partial y}\right) + \frac{\partial}{\partial z}(-nv_z), \tag{1}$$

$$\begin{aligned}\frac{\partial}{\partial t}(nm_\mathrm{i}v_z) = {} & \frac{\partial}{\partial x}\left(\eta_\perp\frac{\partial v_z}{\partial x} + m_\mathrm{i}v_z D\frac{\partial n}{\partial x}\right) \\ & + \frac{\partial}{\partial y}\left(\eta_\perp\frac{\partial v_z}{\partial y} + m_\mathrm{i}v_z D\frac{\partial n}{\partial y}\right) \\ & + \frac{\partial}{\partial z}\left(\eta_\parallel\frac{\partial v_z}{\partial z} + m_\mathrm{i}v_z(-nv_z) - n(T_\mathrm{e} + T_\mathrm{i})\right),\end{aligned} \tag{2}$$

$$\begin{aligned}\frac{3}{2}\frac{\partial}{\partial t}(nT_\mathrm{e,i}) = {} & \frac{\partial}{\partial x}\left(\kappa_\perp^\mathrm{e,i}\frac{\partial T_\mathrm{e,i}}{\partial x} + \frac{5}{2}T_\mathrm{e,i}D\frac{\partial n}{\partial x}\right) \\ & + \frac{\partial}{\partial y}\left(\kappa_\perp^\mathrm{e,i}\frac{\partial T_\mathrm{e,i}}{\partial y} + \frac{5}{2}T_\mathrm{e,i}D\frac{\partial n}{\partial y}\right) \\ & + \frac{\partial}{\partial z}\left(\kappa_\parallel^\mathrm{e,i}\frac{\partial T_\mathrm{e,i}}{\partial z} + \frac{5}{2}T_\mathrm{e,i}(-nv_z)\right) \\ & - K(T_\mathrm{e,i} - T_\mathrm{i,e}).\end{aligned} \tag{3}$$

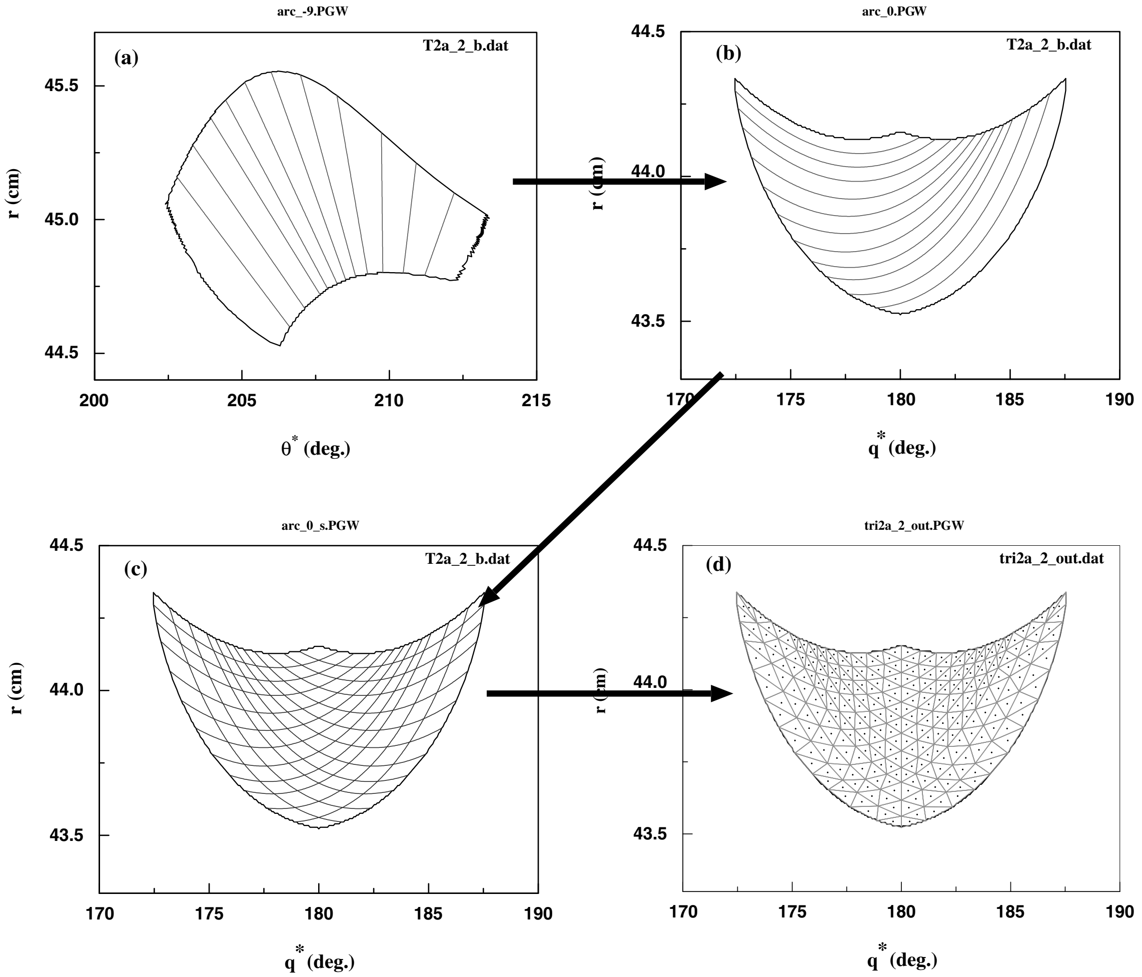

Fig. 2. Optimization of the grid in 2 turn region. (a) The deformed flux tube away from the stagnation plane, where the lines are drawn first. (b) The stagnation plane to where the lines are mapped back. (c) The lines are reflected symmetrically around $\theta = 180°$. (d) The grids are made following the lines.

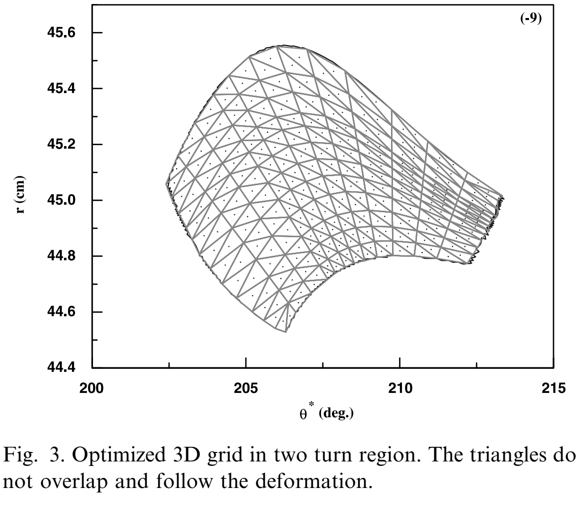

Fig. 3. Optimized 3D grid in two turn region. The triangles do not overlap and follow the deformation.

The flux comes into the SOL at $y = 0$ cm, and no flux is assumed at $y = 4$ cm and at both sides, $x = \pm 1$ cm. The flux is to flow to the wall along the field lines. Eight regularly triangulated grids (128 triangles each) are equally spaced along z for a cross field transport. The calculation started with a initial constant n, v_z, $T_{e,i}$ profiles in both perpendicular and parallel direction except that v_z was set to have smooth increase towards the wall along field lines. The cross field transport calculation is parallelized between the eight cuts and FDM uses an explicit scheme.

The convergence was checked with the area integral of each physical quantity (density, velocity, temperature) at each cut. Fig. 4 shows the time evolutions of the integrals of density and electron temperature. The density decreases toward the wall and takes a maximum around the stagnation point. T_e and T_i are almost constant along

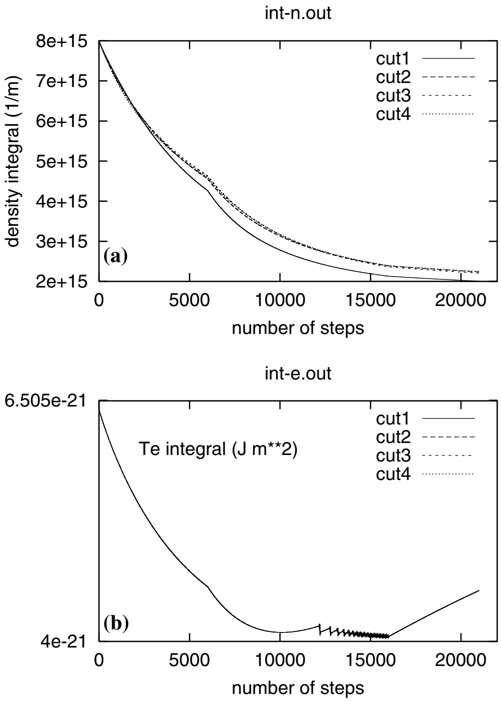

Fig. 4. The time evolutions of area integrals of (a) density and (b) electron temperature at different cuts. The electron temperature starts to oscillate around 12 000 steps. The Δt was set to 2.0×10^{-8} s at first, which was reduced afterwards.

field lines due to the very high heat conductivity $\kappa_{\parallel}^{\mathrm{e,i}}$. In this figure convergence is not reached and we find the integral of electron temperature starts to oscillate around 12 000 step. The oscillation is a precursor to a numerical instability and leads to break down of the calculation.

Since we are using an explicit scheme for parallel transport, the stability is limited in certain parameter domain, which is shown by von Neumann stability analysis. That is, in our case,

$$\Delta t \leqslant \frac{(\Delta z)^2}{2D_{\max}} \propto \frac{(\Delta z)^2 n}{T_{\mathrm{e}}^{2.5}} \tag{4}$$

because, here $D_{\max} = \kappa_{\parallel}^{\mathrm{e}}/1.5n \propto T_{\mathrm{e}}^{2.5}/n$.

The restriction says that one can not predict the future beyond the diffusion time across a cell of width Δz. This threshold is reached around 12 000 steps due to the decrease of n (T_{e} also decreases but that of n is larger). The Δt was reduced to half at 16 000 steps to avoid the instability, then the oscillation stopped and T_{e} started to increase. The increase in T_{e}, however, lowers the threshold in Eq. (4), it forced us to reduce the Δt again afterwards. In the case of Fig. 4, it took 31.4 min. CPU time using eight processors and the particle influx and outflux over the computation domain are not balanced yet ($\sim |\text{influx/outflux}| = 0.63$). We also tried the problem with increased number of triangles (1440, which is necessary for real configuration) using 20 processors, where the convergence was not reached after 50 h. The slow down of the code turns out to be a severe problem.

By using a fully implicit scheme in parallel direction the time step can be selected to be longer and the scheme is unconditionally stable for any time step. However, since we are using a splitting method a physical constraint on the time step arises. For the time step of parallel calculation, $\Delta t_{\parallel}$, it must be smaller than the order of time needed for quantity to propagate across one grid interval in perpendicular direction, i.e., $< (\Delta x_{\perp})^2/(2D)$. For the same argument, the time step of perpendicular calculation, $\Delta t_{\perp}$, must be smaller than the order of $(\Delta x_{\parallel})^2/(2\kappa_{\parallel}^{\mathrm{e}}/n)$, where $\Delta x_{\perp}$ and $\Delta x_{\parallel}$ are a grid spacing in perpendicular and parallel direction, respectively. If we take, $\Delta x_{\perp} \sim 1$ mm, $\Delta x_{\parallel} \sim 1.4$ m, $D \sim 1$ m^2/s, $\kappa_{\parallel}^{\mathrm{e}}/n \sim 3 \times 10^7$ m^2/s, then $\Delta t_{\parallel} < 5 \times 10^{-7}$ s and $\Delta t_{\perp} < 3 \times 10^{-8}$ s, which are almost same order of the time step used in the present analysis.

3.3. Accuracy

A particle balance over the whole computation domain was calculated to check to see the accuracy of the code. For this purpose, the energy equation was skipped. The T_{e} and T_{i} were set constant along the field lines and exponential decay assumed in y direction with $\lambda_T = 2$ cm. Other parameters are same as the problem discussed above. After convergence was reached within about 10 min. CPU time, the particle balance was checked, which is shown in Table 1. The values of DEG indicate the degree of piecewise polynomial basis functions on triangular elements, used in the FEM (Galerkin method) [7]. It is found that changing DEG from 1 to 2 reduces the error significantly with more than 10%, while DEG = 3 and 4 does not so much. The increase of the number of cuts is, surprisingly, not so effective. This is probably due to the rather flat density and velocity profile along the field lines, which is caused by the cross field momentum transport. Concerning the price both for the error and CPU time, second order piecewise basis

Table 1
Particle balance for different DEG, for different number of triangles (128 and 256) and of cuts

DEG	8 cuts	16 cuts		32 cuts
	128	128	256	128
1	80.2 (0.034)	81.0 (0.048)	85.5 (0.069)	81.8 (0.075)
2	95.3 (0.057)	96.7 (0.076)	97.0 (0.127)	98.0 (0.100)
3	95.7 (0.109)	97.1 (0.129)		
4	95.6 (0.194)	97.1 (0.210)		

The values show |influx/outflux| × 100 (%). The values in the brackets are the CPU time per step in seconds.

function (DEG = 2) with fewer triangles would be a reasonable choice for this problem.

4. Summary

The approach to 3D transport simulations for TEXTOR-DED configuration with a FEM has been discussed. In summary:

By introducing the laminar zone, the treatment like SOL model is available and therefore the model becomes rather simple. At the moment, the individual triangles in the 3D grids have about 10% error in the area, which automatically will lead to the error of flux conservation. The cause of the error in the area is the deformation of the flux tube due to the perturbation field. The slow down of the code was found significant due to the explicit scheme used in FDM for parallel transport. The very high heat conductivity in parallel direction, $\kappa_{\parallel}^{e}$, limits the time step. The accuracy of the code was checked with particle balance in a simple straight SOL model, where we found improvement was achieved by a higher degree basis function rather than an increase of number of triangles and of cuts.

Acknowledgement

One of the authors, M.K. is grateful for the financial support by Research Fellowships of the Japan Society for the Promotion of Science for Young Scientists (Cont. no. 0202408).

References

[1] K.H. Finken, G.H. Wolf, Fus. Eng. Des. 37 (1997) 337.

[2] M. Kobayashi, G. Sewell, K.H. Finken, Th. Eich, D. Reiser, S.S. Abdullaev, Contribution Plasma Phys. 42 (2002) 163.

[3] N.A. McTaggert, Proceedings of IEA-DED TEXTOR Workshop, Jülich Germany, 2002 (CD-ROM).

[4] Y. Feng, F. Sardei, J. Kisslinger, D. Reiter, Y. Igitkhanov, Contribution Plasma Phys. 42 (2002) 187.

[5] A. Runov, S. Kasilov, J. Riemann, M. Borchardt, D. Reiter, R. Schneider, Contribution Plasma Phys. 42 (2002) 169.

[6] Th. Eich, D. Reiser, K.H. Finken, Nucl. Fusion 40 (2000) 1757.

[7] G. Sewell, Finite Differences, Finite Elements and PDE2D, self-published, 2000, www.pde2d.com.

[8] J. Wesson, Tokamaks, second ed., Oxford University, New York, 1997, Section 2.23.